Available online at www.sciencedirect.com
SCIENCE DIRECT
ELSEVIER
Solid State Communications 134 (2005) 753–757
solid state communications
www.elsevier.com/locate/ssc

Remarkable improvement of brightness for the green emissions in Ce^{3+} and Tb^{3+} co-activated $LaPO_4$ nanowires

Lixin Yu, Hongwei Song*, Zhongxin Liu, Linmei Yang, Shaozhe Lu, Zhuhong Zheng

Fine Mechanics and Physics, Key Laboratory of Excited State Physics, Changchun Institute of Optics, Chinese Academy of Sciences, 16 Eastern Nan-Hu Road, Changchun 130033, People's Republic of China

Received 29 November 2004; received in revised form 5 March 2005; accepted 14 March 2005 by B. Jusserand
Available online 29 March 2005

Abstract

Ce^{3+} and Tb^{3+} co-activated $LaPO_4$ nanowires (NWs) were synthesized by the hydrothermal method and studied in contrast to corresponding micrometer rods (MRs). The results indicate that electronic transition rate of Ce^{3+} and Tb^{3+} in NWs had only a little variation in comparison with that in MRs, and energy transfer (ET) rate and efficiency of $Ce^{3+} \rightarrow Tb^{3+}$ in NWs reduced. It is interesting to observe that the brightness for $^5D_4$–$^7F_5$ of Tb^{3+} via ET of $Ce^{3+} \rightarrow Tb^{3+}$ in NWs increased several times than that in MRs. This was attributed to the decreased energy loss in excited states being higher than $^5D_4$ of Tb^{3+} ions due to hindrance of boundary.

PACS: 81.07.13c; 78.55.−m; 34.50.Ez

Keywords: A. Nanostructures; E. Luminescence

1. Introduction

One-dimensional (1D) structures, including tubes, wires, rods and belts have aroused remarkable attentions over past decade due to a great deal potential applications, such as data storage [1], advanced catalyst [2], photoelectronic devices [3] and so on. Moreover, in comparison with zero-dimensional (0D) structures, the space anisotropy of 1D structures, provided a better model system to study the dependence of electronic transport, optical and mechanical properties on size confinement and dimensionality [4,5]. With advance in synthesis technique, different morphology 1D materials have been successfully fabricated, such as, SnO_2 nanobelts [5,6], ZnS and ZnO NWs and nanobelts [7,8]. Rare earth (RE) compounds were intensively applied to lighting and display devices. It is expected that the nanosized RE doped phosphors can improve luminescent quantum efficiency and display resolution [9]. Therefore, RE doped nanosized phosphors have attracted considerable attention, for both 1D structures [10–12] and 0D nanoparticles (NPs) [13–15].

Ce^{3+} and Tb^{3+} co-activated $LaPO_4$ bulk powders were extensively applied to fluorescent lamps, cathode ray cube (CRT) and plasma display panel (PDP) because of the high ET efficiency between Ce^{3+} and Tb^{3+} [16,17]. In 1D NWs, how do the electronic transition and the ET processes between Ce^{3+} and Tb^{3+} change in comparison with the bulk crystals? To our knowledge, there is no report on this topic until now. Actually, the studies on ET processes between different RE centers in NWs are quite rare, too. Recently, we successfully fabricated Ce, Tb co-activated $LaPO_4$:NWs as well as MRs by the same method, which permit us to compare their photoluminescent properties. The preparation of $LaPO_4$:RE (RE = Tb^{3+}, Eu^{3+}) NWs by the method was originally reported by Meyssamy et al. [10]. In

* Corresponding author. Tel./fax: +86 431 6176320.
E-mail address: songhongwei2000@sina.com.cn (H. Song).

0038-1098/$ - see front matter © 2005 Elsevier Ltd. All rights reserved.
doi:10.1016/j.ssc.2005.03.026

this paper, we reported the remarkable improvement of brightness in Ce^{3+}, Tb^{3+} co-activated $LaPO_4$ NWs.

2. Experiments

The synthesis of 1D $LaPO_4$ NWs was described in detail in one of our previous papers [18]. In the preparation, appropriate amounts of high purity La_2O_3, $Ce_2(CO_3)_3$ and Tb_4O_7 were dissolved into concentrated HNO_3 firstly and appropriate volume distilled water was added. Then $(NH_4)_2HPO_4$ aqueous solution (0.20 M) was added to the above solution. The final PH value was adjusted to 1–2 with diluted HNO_3 solution (1 M). After vigorously stirred, the milky colloid was poured into several closed Teflon—lined autoclaves and subsequently heated at 120 °C (NWs) and 150 °C (MRs) for 3 h, respectively. The obtained suspension was centrifuged and supernatant was discarded. The resultant precipitation was washed with distilled water and dried at 50 °C at vacuum condition. The dried samples were kept in silicagel desiccator.

Crystal structure, morphology and size were obtained by X-ray diffraction (XRD) using Cu target radiation resource (Cu $K_\alpha = 1.54078$ Å), transmission electron micrograph (TEM) and scanning electron micrograph (SEM) utilizing JEM-2010 electron microscope. Fluorescence and excitation spectra were recorded on a Hitachi F-4500 spectrophotometer equipped with a 150 W Xe-arc lamp at room temperature, and for comparison of different samples, the emission spectra were measured at a fixed band pass of 0.2 nm with the same instrument parameters (2.5 nm for excitation split, 2.5 nm for emission split and 700 V for PMT voltage). In the measurements of fluorescent dynamics of Tb^{3+}, a 355-nm light generated from the Third-Harmonic-Generator pumped by the pulsed Nd:YAG laser was used as excitation source, which was with a line width of 1.0 cm^{-1}, pulse duration of 10 ns and repetition frequency of 10 Hz. The dynamics was recorded by a Spex-1403 spectrometer, a photomultiplier and a boxcar integrator and processed by a computer. The fluorescence lifetime of Ce^{3+} was measured with a FL920 single-photon spectrometer with a nanosecond flashlamp (pulse width: 1 ns; repetition rate: 40 kHz).

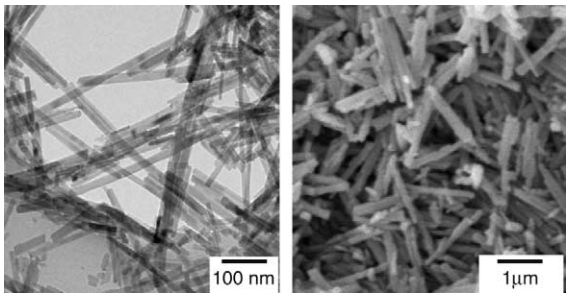

Fig. 1. The TEM of NWs (left) and SEM of MRs (right) images.

3. Results and discussion

Fig. 1 shows TEM and SEM images of $LaPO_4$ powders. From TEM and SEM graphs, the width of NWs prepared at 120 °C is 10–20 nm and length is ~0.5 μm, while the width of MRs prepared at 150 °C is ~200 nm and length is ~2 μm. In fact, the XRD of $LaPO_4$ samples were also measured. Like the bulk $LaPO_4$ polycrystals prepared by the solid reaction, the crystal structure of the two samples belongs to monoclinic monazite type [19]. In our previous work, we proved that the Eu^{3+} entered into $LaPO_4$ NWs lattice by site-selective excitation spectra [20]. In addition, the practical concentration of Eu^{3+} in $LaPO_4$ NWs and MRs was measured and nearly same. Due to similar properties of RE ions, we suggested that Ce^{3+}/Tb^{3+} occupied La^{3+} sites randomly and their practical content was identical in $LaPO_4$:Ce/Tb NWs and MRs.

Fig. 2(a)–(c) show, respectively, the excitation and emission spectra in Ce^{3+}-activated, Tb^{3+}-activated and Ce^{3+}/Tb^{3+} co-activated $LaPO_4$ powders. In Fig. 2(a), the excitation bands consist of three components with maxima at 241, 258 and 276 nm, which are associated with allowed f–d transitions from the ground state $^2F_{5/2}$ to different crystal-field components of 5d level. The emission band consists of two peaks with maxima at 318 and 340 nm, corresponding to the transitions from the lowest 5d excited state to the spin–orbit components (^2D) of the doublet

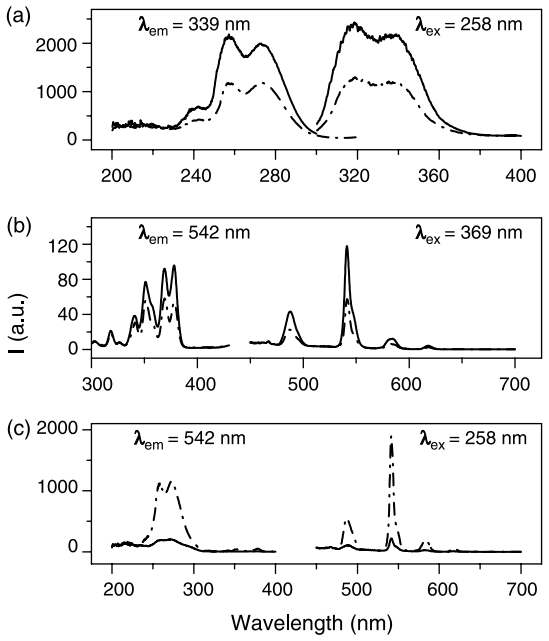

Fig. 2. (a) The excitation (left) and emission spectra (right) of Ce^{3+} in $LaPO_4$:1% Ce powders. (b) The excitation (left) and emission spectra (right) of Tb^{3+} in $LaPO_4$:2.5% Tb powders. (c) The excitation spectra (left) and emission (right) for $LaPO_4$:1% Ce, 2.5% Tb samples. Solid lines and dash dots represented the MRs and NWs, respectively.

ground states, $^2F_{5/2}$, $^2F_{7/2}$. In Fig. 2(b), the excitation lines are associated with $^7F_6$–$^5D_3$, ^5G_J, $^5L_6$ of Tb^{3+}, while the emission lines from 450 to 650 nm are associated with the $^5D_4$–^7F_J ($J=3$–6) transitions. According to Fig. 2(a) and (b), in Ce^{3+}-activated and Tb^{3+}-activated samples, the fluorescence intensity in NWs was lower than that in MRs. In Fig. 2(c), as monitoring the emission of Tb^{3+} at 542 nm, the strong allowed f–d transitions of Ce^{3+} and the weak forbidden f–f transitions of Tb^{3+} ions were observed, implying efficient ET from Ce^{3+} to Tb^{3+} ions. The intensity of Tb^{3+} originated from Ce^{3+}–Tb^{3+} ET excitation is two-order higher than that from the f–f transitions of Tb^{3+}.

Fig. 3(a) and (b) show, respectively, the dependence of the $^5D_4$–$^7F_5$ emission intensity of Tb^{3+} from Ce^{3+}–Tb^{3+} ET excitation and the ET efficiency of $Ce^{3+}\rightarrow Tb^{3+}$ on concentration of Tb^{3+} in $LaPO_4$:Ce^{3+}/Tb^{3+} powders. The ET efficiency from a donor (Ce^{3+}) to an acceptor (Tb^{3+}) was calculated according to the formula $\eta_{ET}=1-I_d/I_{d0}$, where I_d and I_{d0} were the corresponding luminescence donor intensity in the presence and absence of the acceptor for the same donor concentration, respectively. The ET efficiency for both NWs and MRs increased with Tb^{3+} concentration, and that in NWs increased more rapidly. The ET efficiency in NWs decreased than that in MRs for any Tb^{3+} concentrations. Despite the ET efficiency in NWs decreased, the brightness of Tb^{3+} increased 3–5 times in comparison with that in MRs.

In Ce^{3+}/Tb^{3+} co-activated materials, the brightness of Tb^{3+} via ET excitation was dominated by the following factors: (1) the electronic transition rate and the density of Ce^{3+}, (2) the ET efficiency of $Ce^{3+}\rightarrow Tb^{3+}$, and (3) the electronic transition rate and density of Tb^{3+}. To determine the electronic transition rate and the ET rate, the fluorescent dynamics of Ce^{3+} and Tb^{3+} were investigated. Fig. 4 shows the dependence of fluorescent lifetimes of Ce^{3+} on (a) Ce^{3+} concentration and (b) Tb^{3+} concentration. In Fig. 4(a), as the concentration of Ce^{3+} varied from 0.25 to 2.5% in molar ratio, the lifetime of Ce^{3+} in NWs hardly changed, while in MRs that decreased with increasing Ce^{3+} concentration. This indicated that the extinction concentration for NWs was higher than that for MRs. Similar results were also observed in NPs [21]. In nanosized materials, due to the limited number of primitive cells per particle, on average there are only a few traps in one particle, so the traps distribute randomly with a considerable large fluctuation among particles. Some particles may contain many traps while others may contain no trap at all. The energy of a luminescence center can only be transferred resonantly within one particle since the ET is hindered by the particle boundary [21]. Therefore, quenching occurs at higher concentration in nanosized materials than in normal materials. In addition, according to Fig. 4(a), the cross-relaxation among Ce^{3+} ions for 1% concentration hardly took place. In Fig. 4(b), the lifetime of Ce^{3+} in both NWs and MRs decreased with the concentration of Tb^{3+} and in MRs it decreased more rapidly. The reverse of the lifetime of Ce^{3+} was well fitted with a linear function $\tau^{-1}\propto R_C+R_{ET}\times[Tb^{3+}]$, where R_C is the electronic transition

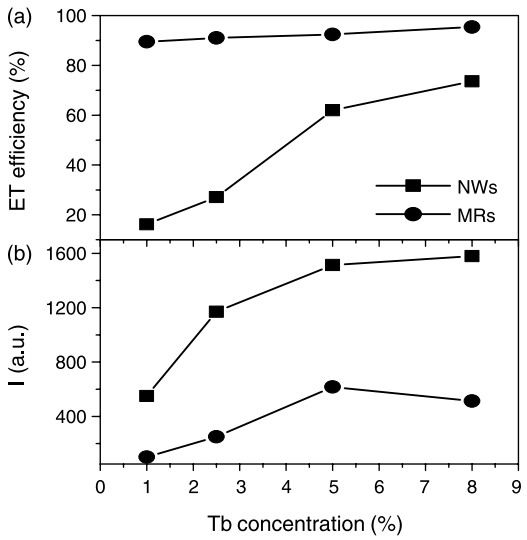

Fig. 3. The dependence of ET efficiency (a) and emission intensity of Tb^{3+} at 258 nm excitation (b) on the Tb^{3+} concentration for the same Ce^{3+} concentration (1%).

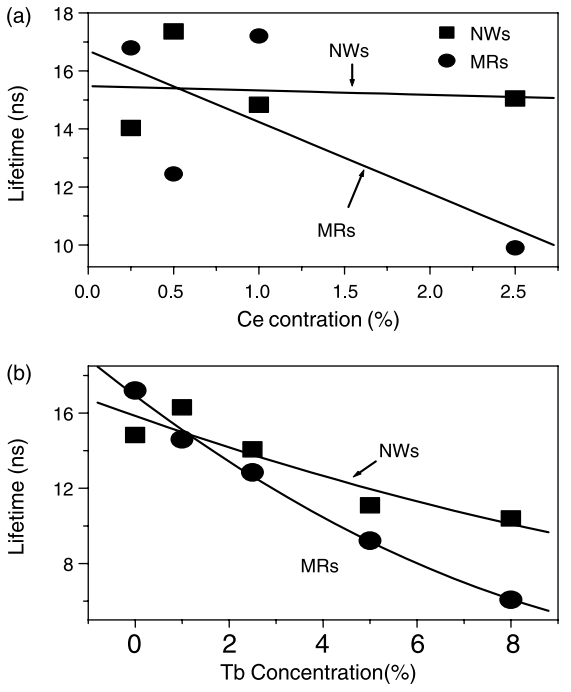

Fig. 4. The dependence of Ce^{3+} lifetimes on Ce^{3+} concentration for singly doped Ce^{3+} samples, (a) and on Tb^{3+} concentration for the same Ce^{3+} content (1%) monitoring 355 at 272 nm excitation, (b) scattered dots were experimental dots and solid lines were fitted curves.

rate of Ce^{3+}, including the radiative and non-radiative transitions, and R_{ET} is the total ET rate of $Ce^{3+} \rightarrow Tb^{3+}$. R_C was determined, to be $6.3 \times 10^{-2}\ ns^{-1}$ in NWs, and $5.2 \times 10^{-2}\ ns^{-1}$ in MRs. R_{ET} was deduced, to be $0.44\ ns^{-1}mol^{-1}$ in NWs and $1.30\ ns^{-1}mol^{-1}$ in MRs. The electronic transition rate of Ce^{3+} in NWs increased a little than that in MRs, while the ET rate of $Ce^{3+} \rightarrow Tb^{3+}$ in NWs decreased nearly three times. The $^5D_4$–$^7F_5$ fluorescence decays of Tb^{3+} in $LaPO_4$:2.5% Tb NWs and MRs were also compared. The exponential lifetime was determined, to be 2.72 ms in NWs and 2.57 ms in MRs. This indicates that the total electronic transition rate of $^5D_4$ hardly changes in NWs and MRs. In addition, the lifetime of $^5D_4$–$^7F_5$ lines at different temperatures hardly changes, indicating that the non-radiative relaxation via $^5D_4$ can be ignored, and the reverse of lifetime equals to the radiative transition rate of $^5D_4 \rightarrow \sum {}^7F_J$, to be $0.37\ ms^{-1}$ in NWs and $0.39\ ms^{-1}$ in MRs. In addition, the extinction role of absorbed water at the surface should be considered [22]. There existed more absorbed water at the surface. In NWs due to surface effect. If the absorbed water played a role of extinction, the intensity of Tb^{3+} in NWs should decrease in contrast to MRs. However, the present results were opposite this point. We can exclude the effect of extinction from absorbed water.

The electronic transition rate for Ce^{3+} or Tb^{3+} in NWs and MRs had only a little variation, and the ET rate of $Ce^{3+} \rightarrow Tb^{3+}$ in NWs decreased three times than that in MRs. The density variation of Ce^{3+} and Tb^{3+} ions in NWs and MRs can be also neglected. Surprisingly, the brightness of $^5D_4 \rightarrow {}^7F_5$ emissions in Ce^{3+}/Tb^{3+} co-activated NWs increased. In $LaPO_4$:Ce, Tb as exciting Ce^{3+} ions, electrons were excited from the ground state, $^2F_{5/2}$ to 5d excited state of Ce^{3+} and then feed to some excited states of Tb^{3+}. The electrons at higher excited states relax to $^5D_4$ and generate $^5D_4$–$^7F_5$ transitions. According to the energy levels of Ce^{3+} and Tb^{3+} and the theory of Foster–Dexter, the ET from Ce^{3+} to the $^5H_6$ level of Tb^{3+} has the largest probability. We suggested that at higher excited states than $^5D_4$ some energies loosed through some ET, which caused the electron population reaching $^5D_4$ to decrease. Fig. 5 shows the decay curves of $^5D_3$–$^7F_5$ of Tb^{3+} in the NWs and MRs. The decay curve included two components, a faster and a slower, for both NWs and MRs and was well fitted by a function of $I_1\exp(-\tau_1/t)+I_2\exp(-\tau_2/t)$, where $I_1+I_2=1$. The fitting parameters are $I_1=0.23$, $\tau_1=7.3$ μs, $I_2=0.77$ and $\tau_2=68$ μs for NWs and $I_1=0.62$, $\tau_1=6.8$ μs, $I_2=0.38$ and $\tau_2=84$ μs for MRs. The decay constants of the two components changed not much. But the relative proportion of two components varied greatly. In NWs the slower component is dominant, while in MRs the faster component is dominant. On one hand, the electrons in the higher excited states can non-radiatively relax to the lower excited states. On the other hand, if there exist some defect states near Tb^{3+}, the energies of the-higher-excited-state-electrons can transfer to the defect states and electrons non-radiatively transit to the ground states. Because the non-radiative ET rate between a luminescent center of RE and a defect level nearby is much faster than the non-radiative relaxation rate of RE [23,24], it was proposed that the two components for the $^5D_3$–$^7F_5$ transitions corresponded to two processes, the slower to the non-radiative relaxation of $^5D_3$–$^5D_4$ and the faster to the ET from $^5D_3$ to some defect levels. In MRs, although more Tb^{3+} ions are excited to excited states through the ET of $Ce^{3+} \rightarrow Tb^{3+}$, most of them non-radiatively transit to the ground state again through the ET of Tb^{3+} to the defect levels. In NWs, despite less Tb^{3+} ions are excited to excited states, most of them generate $^5D_4$–^7F_J emissions because the ET processes of $Tb^{3+} \rightarrow$ defect levels in higher excited states decreased. Therefore, the brightness for the green emissions of Tb^{3+} in NWs increased. This can be still attributed to the hindrance of the more boundary in NWs.

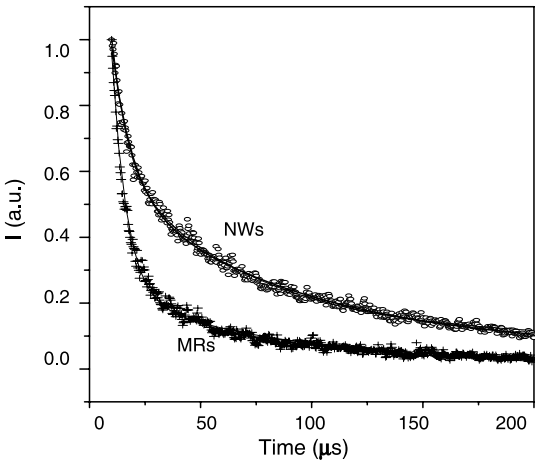

Fig. 5. The decay curves of $^5D_3$ of Tb^{3+} in $LaPO_4$:2.5% Tb NWs and MRs monitoring 414 at 355 nm excitation.

4. Conclusions

In conclusion, $LaPO_4$:Ce/Tb NWs and the corresponding MRs were fabricated by the hydrothermal method and their photoluminescent properties were compared. The results indicate that in NWs the ET rate and efficiency from Ce^{3+} to Tb^{3+} became lower than that in MRs, but the brightness of the green $^5D_4$–$^7F_5$ emission through ET excitation increased 3–5 times. This was contributed to decreased energy loss from the higher level than $^5D_4$ of Tb^{3+} ions due to the hindrance of the boundary.

Acknowledgements

The authors gratefully thank the financial supports of One-Hundred Project from Chinese Academy of Sciences

and Nation Natural Science Foundation of China (Grant No. 10374086 and 10274083).

References

[1] Y. Kong, D. Yu, B. Zhang, W. Fang, S. Feng, Appl. Phys. Lett. 78 (2001) 4.
[2] X. Daun, Y. Yang, Y. Cui, J. Wang, C. Lieber, Nature 409 (2001) 66.
[3] Z. Pan, Z. Dai, Z. Wang, Science 291 (2001) 1947.
[4] M. Huang, S. Mao, H. Feick, H. Yan, Y. Wu, H. Kind, E. Weber, R. Russo, P. Yang, Science 292 (2001) 1897.
[5] Y. Xia, P. Yang, Adv. Mater. 15 (2003) 351.
[6] X. peng, L. Zhang, G. Meng, Y. Tian, Y. Lin, B. Geng, S. Sun, J. Appl. Phys. 93 (2003) 1760.
[7] X. Wang, P. Gao, J. Li, C. Summers, Z. Wang, Adv. Mater. 14 (2002) 1732.
[8] J. Choy, E. Jang, J. Won, J. Chung, D. Jang, Y. Kim, Appl. Phys. Lett. 84 (2004) 287.
[9] R. Bhargava, D. Gallagher, X. Hong, Phys. Rev. Lett. 72 (1994) 416.
[10] H. Meyssamy, K. Riwotzki, Adv. Mater. 11 (1999) 840.
[11] M. Yada, M. Mihara, S. Mouri, T. Kijima, Adv. Mater. 14 (2002) 309.
[12] X. Wang, Y. Li, J. Eur. Chem. 9 (2003) 5627.
[13] R.S. Meltzer, S.P. Feofilov, B. Tissue, Phys. Rev. B 60 (1999) R14012.
[14] D.K. Williams, B. Bihari, B.M. Tissue, J.J.M. McHale, J. Phys. Chem. B 102 (1998) 916.
[15] H. Song, B. Chen, H. Peng, J. Zhang, Appl. Phys. Lett. 81 (2002) 1776.
[16] J. Dexpert-Ghys, R. Mauricot, M.D. Faucher, J. Lumin. 69 (1996) 203.
[17] X. Wu, H. You, H. Gui, X. Zeng, G. Hong, C. Kim, C. Pyun, B. Yu, C. Park, Mater. Res. Bull. 37 (2002) 2531.
[18] H. Song, L. Yu, S. Lu, Z. Liu, L. Yang, Appl. Phys. Lett. 85 (2004) 470.
[19] U. Rambabu, S. Buddhudu, Opt. Mater. 17 (2001) 401.
[20] L. Yu, H. Song, S. Lu, Z. Liu, L. Yang, X. Kong, J. Phys. Chem. B 108 (2004) 16697.
[21] Z. Wei, L. Sun, C. Liao, J. Yin, X. Jiang, C. Yan, J. Phys. Chem. B 106 (2002) 10610.
[22] H. Song, J. Wang, B. Chen, S. Lu, Chem. Phys. Lett. 376 (2003) 1.
[23] S. Huang, L. Lou, J. Lumin. 45 (1990) 377.
[24] L. Lou, S. Huang, J. Lumin. 40/41 (1988) 667.